
CORRELATION ANALYSIS OF SOLAR FLUX ABSOLUTE MEASUREMENTS AT 161 AND 245 MHz

A.G. Setov

*Institute of Solar-Terrestrial Physics SB RAS,
Irkutsk, Russia, setov@iszf.irk.ru*

D.S. Kushnarev

*Institute of Solar-Terrestrial Physics SB RAS,
Irkutsk, Russia, ds_k@iszf.irk.ru*

Abstract. Solar emission in meter waves originates from upper layers of the solar corona. We present absolute measurements of solar flux from Irkutsk Incoherent Scatter Radar (161 MHz frequency) and Learmonth Observatory (245 MHz frequency). We perform correlation analysis to investigate the relation between solar flux values at different frequencies. Background emission of the quiet Sun is within the expected limits. We examine the behavior of background and slowly-varying emission components during a solar cycle. By comparing the Pearson correlation coefficient with the Spearman rank correlation coefficient, we have found that the dependence of the meter flux on the $F10.7$ index is non-linear. The correlation between solar flux measurements

at 161 and 245 MHz appeared to be lower than that with the $F10.7$ index. Analysis of daily correlation and auto-correlation shows a diurnal variation that introduces an error into the measurements.

Keywords: solar emission, absolute measurements, Irkutsk Incoherent Scatter Radar (IISR), Learmonth Observatory, meter waves, background emission, slowly-varying component.

INTRODUCTION

Solar emission covers the entire radio frequency spectrum, and the mechanism of its occurrence and influence on the Sun–Earth system varies significantly with frequency. To date, many instruments have been developed to observe solar emission, but VHF emission is less frequently studied [Borkowski, 1982; Lantos, 1998; Iwai et al, 2012]. In this range, the emission source is located in the solar corona. The dominant mechanism of emission depends on solar activity: for the quiet Sun, it is thermal bremsstrahlung; during radio bursts (sharp increases in emission intensity), non-thermal emission at the plasma frequency, its harmonics, or gyrofrequency harmonics. Recently, new large calibrated radio telescopes in the range to 300 MHz have appeared — LOFAR (LOW Frequency Array) [Vocks et al., 2018] and MWA (Murchison Widefield Array) [Oberoi et al., 2017], which, however, explore the Sun only in individual experiments. Nonetheless, the instrumental coverage of meter waves leaves much to be desired. Moreover, to extensively study emission and spectral distribution, as well as to compare data from different instruments, it is necessary that solar emission measurements be absolute, i.e. a specific physical value is obtained by a calibrated instrument [Tapping, 2013; Lu et al., 2015; Tan et al., 2015].

General estimator of the level of solar emission is the spectral flux density of solar emission, briefly called the total flux. This value is measured in solar flux units (s.f.u.). In this paper, we conduct a correlation analysis to study the relationship between solar fluxes at different meter wave frequencies in a solar cycle and make a comparison with the $F10.7$ index. We present solar flux

measurements performed with the Irkutsk Incoherent Scatter Radar (IISR) at a frequency of 161 MHz and at Learmonth Observatory at a frequency of 245 MHz. The choice is due to geographical location: IISR is located at 120 km from Irkutsk (103° E); Learmonth, in Australia (114° E); therefore, they can observe the Sun at about the same time. IISR data covers the period from 2011 to 2022; Learmonth data, from 2006 to 2022.

Since 1990s, IISR operating in 154–163 MHz has been used to solve various scientific problems [Medvedev, Potekhin, 2019] such as ionospheric research, detection and tracking of space objects, radio astronomy observations. IISR has also been used in a number of special experiments: observation of coherent echoes from field-aligned irregularities; study of ionospheric irregularities occurring when Progress spacecraft engines worked, and radiosounding of the Moon. Location of the radar is unique because it is the only such scientific instrument in Eastern Siberia. During the spring-summer period, the radar makes observations of the Sun and solar emission flux measurements at 161 MHz ($\lambda=1.86$ m). They are of interest because there are few radio telescopes in the world that can perform absolute measurements in meter waves with high sensitivity. The radar receiver has been calibrated and a solar flux measurement method for several observation modes has been developed [Setov et al., 2020]. Here we examine the statistical features of the solar flux data compared to the data from Learmonth Observatory.

Learmonth Observatory is part of the Radio Solar Telescope Network (RSTN), which performs regular absolute measurements of solar flux at eight discrete frequencies. RSTN data is often used for studying the

behavior of solar emission in a wide frequency range [Kashapova et al., 2021], as well as for calibrating other scientific instruments [Hamini et al., 2021] and telecommunication systems [Giersch, Kennewell, 2022]. Giersch and Kennewell [2022] have carried out a correlation analysis of data between different RSTN stations and described measurement errors at different frequencies.

We describe in detail methods of processing IISR data, examine the behavior and statistical characteristics of mean annual, mean daily, and diurnal solar fluxes at 161 and 245 MHz. In addition, we compare solar flux distribution during the quiet Sun with expected model values. At the end of the paper, we investigate the auto-correlation of measurements for neighboring days and the source of measurement errors — the unexplained diurnal variation.

1. DATA PROCESSING METHODS

IISR has a horn antenna of size 246×12 m and of height ~20 m [Potekhin et al., 2009; Medvedev, Potekhin, 2019]. The antenna beamwidth is $0.5^\circ \times 10^\circ$. In the horn there is a polarization filter consisting of metal strips and passing only one (horizontal) polarization. The long side of the antenna is oriented north—south. At the base of the antenna is a trench structure with feed horns at the input and output. The antenna pattern beam direction is determined by the frequency of the exciting wave. Changing the frequency from 154 to 163 MHz leads to a 30° southward beam steering. This limits the bandwidth of signals received from a certain direction. Since a 200 kHz band is used to measure the solar flux, the effective beamwidth is $1.25^\circ \times 10^\circ$.

The Sun enters the IISR field of view in the spring-autumn period and is observed in the main beam from May 1 to August 15. As the Sun passes through the field of view, the frequency at which the signal is maximum varies from 159 to 163 MHz, but we will refer the resulting solar flux to the frequency of 161 MHz — the mean frequency of observing the Sun at the antenna pattern maximum. The measurements are carried out in radio astronomy mode when the radar transmitter system is completely disabled. Most measurements are made in the period from 03:30 to 07:30 UT (from 10:30 to 14:30 LT).

The method of estimating the solar flux from IISR data involves filtering and averaging a received signal, calibrating radar receiver and antenna pattern, and directly calculating the total flux. In this paper, we deal with the background and slowly-varying components of solar emission and filter out short-term radio bursts lasting to 1 min. The background component corresponds to the quiet Sun's emission when there are no sunspots on the disk. The slowly-varying component represents long-term increases in the level of solar emission when active regions appear on the Sun's surface. Short-term radio bursts and electromagnetic interference are filtered through threshold filtering, using median absolute deviation that is more resistant to intense outliers than the standard deviation. After the filtering and averaging, the time resolution is 1 s.

To calibrate the IISR receiver, we have long used [Setov et al., 2018, 2020] sky noise maps obtained for

a specific frequency by the model of diffuse galactic radio emission [Zheng et al., 2016]. The calibration is performed as follows: a signal at each individual frequency is compared with a model signal to determine the frequency response and the noise temperature of antenna—receiver system. The calibration allows us to determine the received signal power in watts.

The novelty of this work is an additional correction of the antenna pattern made using an archive of solar observations. According to the results of comparison between waveforms (tracks) for the same day and month, but for different years, the true antenna pattern shape at frequencies above 159 MHz proved to differ significantly from the model one and change considerably with frequency. To correct the diagram, we have chosen a reference track of the Sun corresponding to the quiet Sun for each combination of day and month, and have normalized it. Then, the antenna pattern was adjusted in accordance with the reference track for a particular day of observation. In addition, we corrected the temperature dependence. Since the antenna is large and is subject to temperature expansion and compression, strong temperature gradients of the sharp continental climate of Eastern Siberia cause coefficients of the scanning equation to change. A peak signal from radio sources is shifted in frequency. To compensate for the shift, we fit the Gaussian to the spectrum of the received signal at the processing stage. Additional adjustments to the antenna pattern allowed us to increase the duration of daily measurements and the total number of days of solar flux measurement compared to earlier works.

The received signal power P_r has the form

$$P_r = \frac{\lambda^2}{8\pi} \int \int_{\Omega_B} I(\theta, \varphi) F(\theta, \varphi, f) G(f) df d\Omega, \quad (1)$$

where I is the radio source intensity; F is the antenna pattern; G is the gain; B is the receiver bandwidth; Ω is the solid angle; λ is the wavelength.

To calculate the solar flux, we assume that angular dimensions of the Sun are small compared to the effective beamwidth for a signal with $B=200$ kHz. Then (1) can be simplified:

$$P_r = \frac{\lambda^2}{8\pi} G_0(\theta_0, \varphi_0) S_{\text{sun}}, \quad (2)$$

where G_0 is the gain at (θ_0, φ_0) ; S_{sun} is the desired solar flux (the intensity integral over the solar disk).

In (2), the received flux is doubled to account for the effect of the linear polarization filter in the antenna. This approach is often adopted when calculating the solar flux in meter waves since the solar background emission is not polarized in it, and during radio bursts the emission has circular polarization, which for an antenna with linear polarization leads to the same reduction in the received power by half.

A random measurement error is estimated by the error propagation method. It is assumed that received signal quadratures have a Gaussian distribution. It has been found that for 92 % of flux measurements the relative standard deviation is lower than 10 %; for 98 % of the measurements, lower than 20 %. The systematic measurement error includes the diurnal variation in data se-

ries (discussed in more detail below), calibration errors, and errors due to assumptions made when calculating the solar flux. It is difficult to accurately estimate the effect of the systematic error, but comparative analysis of data for different years allows us to assume that the error is 5–25 %.

RSTN consists of four stations spaced so as to ensure continuous observation of the Sun. The stations have a standard set of antennas for recording solar emission at eight discrete frequencies from 245 to 15400 MHz [Giersch, Kennewell, 2022]. Learmonth Solar Observatory, located in Australia, has a variety of instruments for studying the Sun, including RSTN antennas. In this paper, we are interested in Learmonth measurements of solar flux at 245 MHz, available on the website [https://www.sws.bom.gov.au/Solar/3/4]. At this frequency, a log-periodic antenna with a size of 8.5 m and a beam width of 10° is used. Absolute measurements are carried out mainly from 22:00 to 10:00 UT and have a time resolution of 1 s. When processing the data, we filtered out the flux values smaller than 2 s.f.u. and above 10000 s.f.u.

The correlation analysis is based on the Pearson correlation coefficient R as a measure of the linear dependence of two random variables and the Spearman (rank) correlation coefficient S [Spearman, 1904], which shows how well the relationship between two random variables can be described by a monotonic function. When determining the Spearman coefficient, initial data series are replaced with ranks — ordinal numbers of measurements in samples sorted in ascending order. Next, the Pearson correlation between the sets of ranks is calculated by a simplified formula

$$s = 1 - \frac{6}{n(n-1)(n+1)} \sum_{i=1}^n (R_i(X) - R_i(Y))^2, \quad (3)$$

where $R_i(X)$, $R_i(Y)$ are the ranks of the i -th measurement in samples X and Y ; n is the size of the samples. We utilize the Spearman coefficient as a more general metric of correlation between two values, not limited only by linear dependence.

2. STUDYING MEAN ANNUAL VARIATIONS IN A SOLAR CYCLE AND DISTRIBUTIONS OF MEAN DAILY FLUXES

Figure 1 plots the mean annual solar flux at frequencies of 161 and 245 MHz in 2006–2022 as a function of sunspot number. Table at the bottom of the plot shows the number of days per year in which the flux measurements were carried out. For IISR data, the total number of days is 643 days; for Learmonth data, 5458 days. IISR makes measurements only in spring and summer and alternates them with active ionospheric and satellite observations, whereas Learmonth instruments are designed for round-the-clock monitoring of solar activity. In 2014–2016, IISR made almost no measurements. Figure 1 shows that the solar flux in meter waves increases with increasing solar activity. It seems that the new cycle will be more active in VHF because the flux at 245 MHz in 2021–2022 has already exceeded the values of the last cycle (2008–2019), as well as the flux at 161 MHz in 2022 exceeded that in 2011.

The flux at 161 MHz exceeded that at 245 MHz in 2012, 2013, and 2015, although it is theoretically expected that the flux should increase with frequency at least for the quiet Sun [Benz, 2009]. For 2015, the difference is due to a small sample of data — in a short 14-day period from June 19, 2015 to July 02, 2015, a strong radio storm was observed (a long, sometimes multi-day, solar flux increase). In 2011–2013, IISR worked in the former mode that did not allow for effective filtering of interference and could introduce an error in measurements. On the other hand, during years of high solar activity, the mean annual flux at 161 MHz could be higher due to the fact that radio storms were more intense at this frequency. To estimate the difference between 161 and 245 MHz, we have constructed histograms of the mean daily flux (Figure 2). The distribution over the entire observation period exhibits a variety of solar flux values from a few to hundreds of s.f.u. The

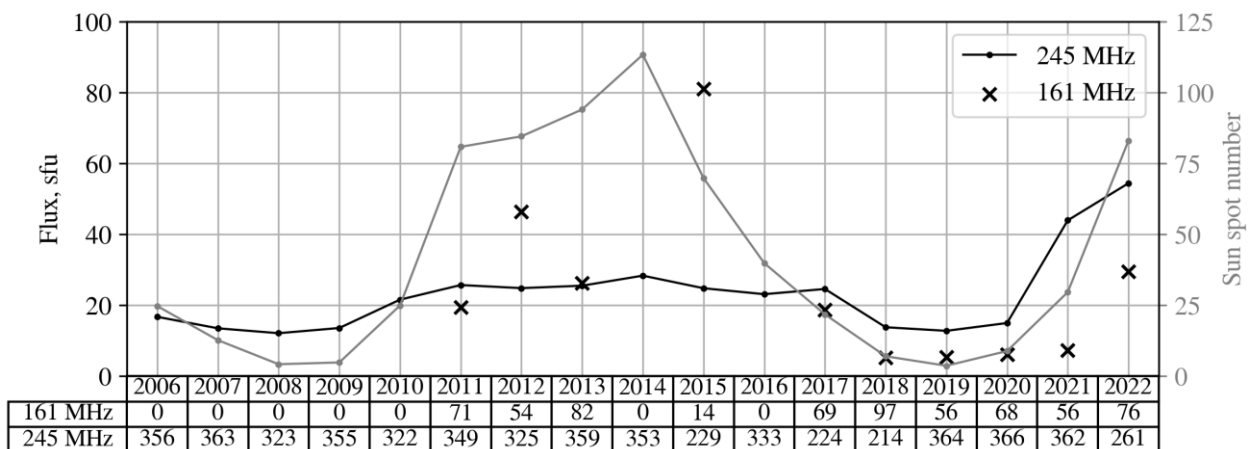


Figure 1. Mean annual solar flux and mean annual sunspot number. The black line is a flux at a frequency of 245 MHz; black crosses mark a flux at a frequency of 161 MHz; the gray line is the sunspot number. The X-axis is the total number of days of solar observation at the corresponding frequency

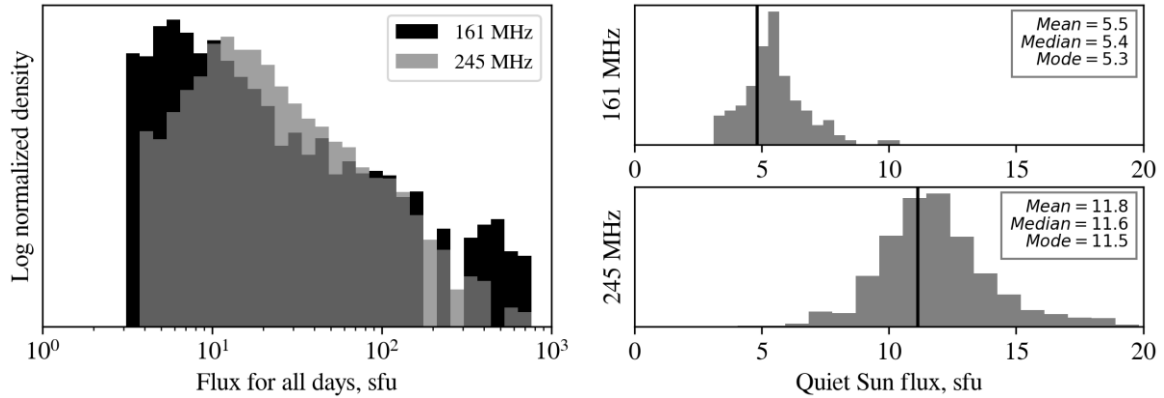


Figure 2. Mean daily solar flux for the entire observation period on a logarithmic scale (left); for the quiet Sun (right). The black vertical line indicates a model quiet-Sun flux according to [Benz, 2009]

distribution mode at 161 MHz is expected to be lower than that at 245 MHz, but the IISR measurements have a large number of extreme values (above 200 s.f.u.)

The mean annual flux (see Figure 1) is the sum of the background emission and the slowly-varying emission component. The background solar emission can further be measured when there are no sunspots on the solar disk. In two right panels (see Figure 2) are histograms of the quiet-Sun flux. We have selected the days when the number of sunspots is zero on the day of observation, the day before and after the day of observation: 124 days for IISR data (19 % of all data), 1416 days for Learmonth (22 % of all data). The measurements are compared with the model quiet-Sun flux (vertical lines) according to [Benz, 2009], where the formula approximating the flux at solar minimum is given. The model values are 4.8 s.f.u. for 161 MHz and 11.1 s.f.u. for 245 MHz. Hamini et al. [2021] have modified the formula [Benz, 2009] based on data from the San Vito RSTN station in order to approximate the solar flux during solar maximum (8.1 s.f.u. for 161 MHz and 18.8 s.f.u. for 245 MHz). However, quiet days are more often observed at solar minimum, and the sample for solar maximum is unrepresentative. Thus, the IISR and Learmonth quiet-Sun fluxes are close to the expected values during solar minimum (the mean, median, and mode of distributions are shown in Figure 2).

3. CORRELATION ANALYSIS OF MEAN DAILY FLUXES

We have carried out a correlation analysis, using data on the mean daily solar flux. Averaging has been made over all data for each day. Duration of solar flux measurements for each selected day is at least 1 hr; with the average duration of Learmonth measurements ~ 10 hrs; IISR, ~ 3 hrs.

When calculating the correlation, outliers that introduce an error in the estimate are usually eliminated. As it has been shown above, the VHF solar flux varies by two orders of magnitude; it is therefore interesting to study the correlation dependence on the outlier cutoff threshold. Figure 3 illustrates the Pearson and Spearman correlation matrices between the 161 MHz flux, $F_{10.7}$ (2800 MHz) [Tapping et al., 2013] and the 245 MHz flux. In each cell of the matrix, the corresponding Pear-

son or Spearman coefficient is calculated from the part of the sample where flux values are equal to or below a certain threshold (percentile).

Comparing the 161 MHz flux and $F_{10.7}$ (top panels) shows that the Pearson correlation is the highest $R=0.7\pm 0.74$ for the 161 MHz flux values below 14 s.f.u. (80 % of the data). At the same time, the Spearman correlation is maximum $S=0.79$ when using all available data, which suggests that the relationship between the fluxes is non-linear. The correlation matrix between 245 MHz and $F_{10.7}$ (not shown in Figure) has an identical distribution with the Pearson correlation maximum $R=0.67$ for the 245 MHz flux values below 24.7 s.f.u. (80 %) and with a sharp decrease in the Pearson correlation to $R=0.25$ when using all data with $S=0.71$. A sharp decrease in the Pearson correlation to $R=0.2\pm 0.4$ for the 100 % percentile with a slight change in the Spearman correlation suggests that a large increase in the 161 and 245 MHz fluxes is not accompanied by a significant change in the $F_{10.7}$ flux. A similar comparison of the 161 and 245 MHz fluxes with the sunspot number has revealed that both Pearson and Spearman correlations are by ~ 0.1 lower than the correlation with $F_{10.7}$.

Comparing the 161 and 245 MHz fluxes (bottom panels) has shown two features. Firstly, the Pearson correlation is maximum when all data is used. First of all, this is due to noise storms that are observed simultaneously at both frequencies and have fluxes above 100 s.f.u. The second feature stems from the fact that the maximum Pearson and Spearman correlation coefficients ($R=0.71$, $S=0.71$) are unexpectedly lower than those in the correlation matrix with $F_{10.7}$, despite the proximity of meter-wave frequencies. Estimated correlation may have an error since daily Learmonth measurements have a longer duration; therefore, short-term increases in the 161 MHz flux can cause an error in the estimated mean daily flux, whereas averaging of 245 MHz measurements better smooths out single peaks.

4. CORRELATION ANALYSIS OF DIURNAL FLUX VARIATIONS

Due to the close longitude location and the 1 s time resolution, we can directly compare the flux measurements at two frequencies obtained during the day. Figure 4

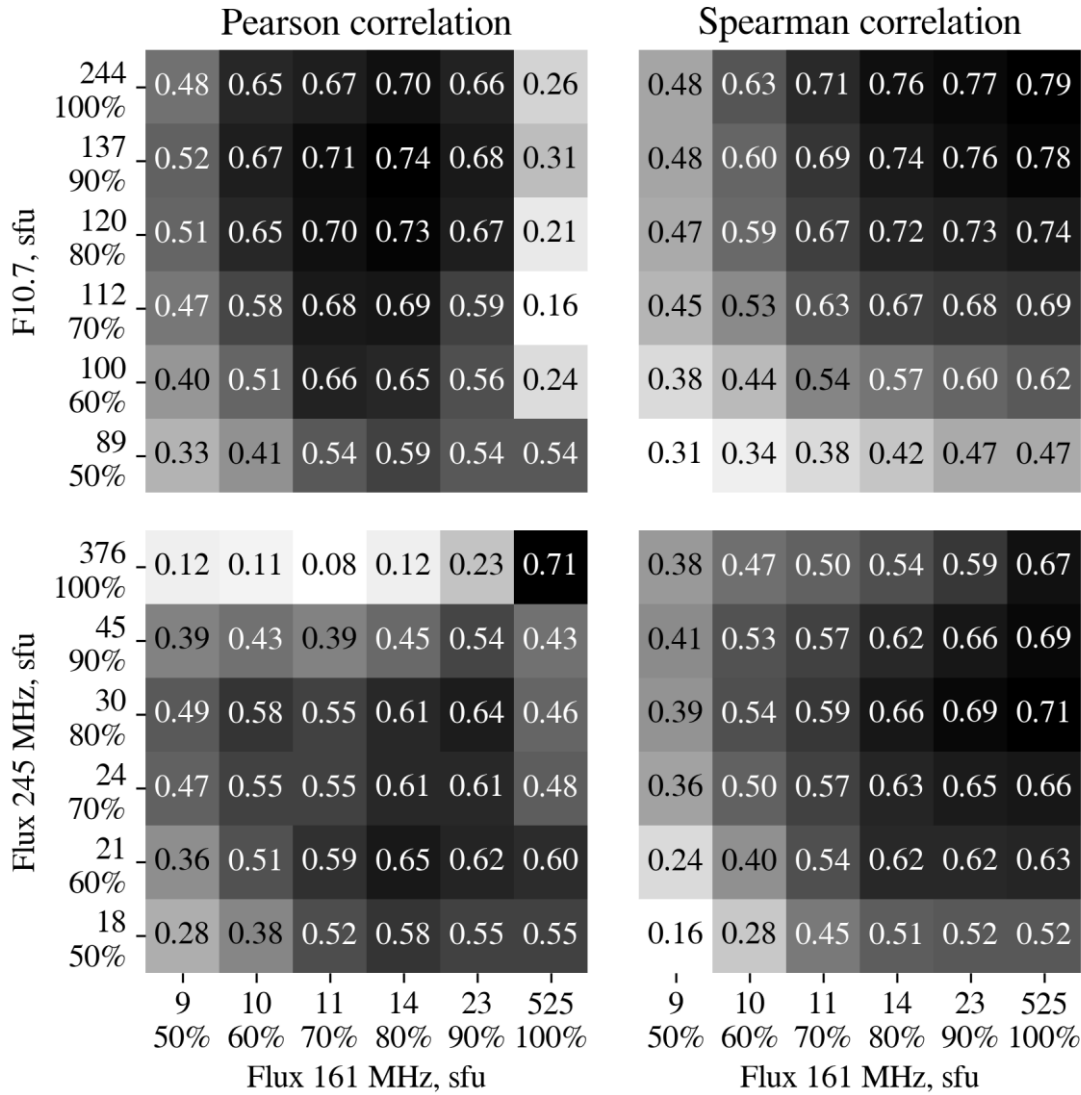


Figure 3. Correlation matrices of a mean daily flux at different percentiles of data samples. The top row is the correlation between the 161 MHz flux and F10.7. The bottom row is the correlation between the 161 and 245 MHz fluxes. On the left is the Pearson correlation; on the right, the Spearman correlation

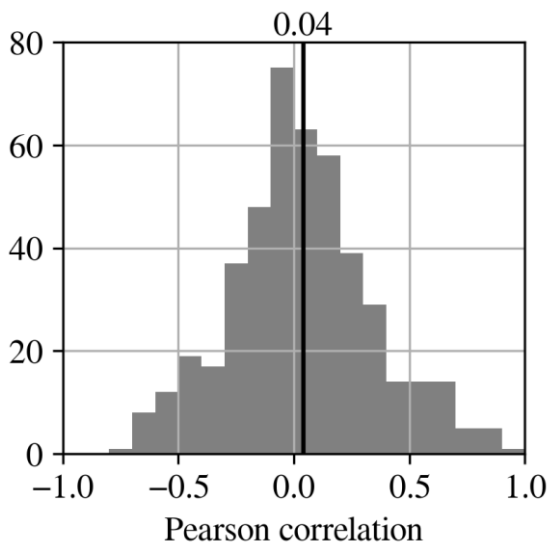


Figure 4. Pearson correlation between diurnal flux variations at 161 and 245 MHz. The vertical black line indicates the mean correlation coefficient

presents a histogram of the Pearson correlation between diurnal variations in the 161 and 245 MHz fluxes. The distribution has a Gaussian shape with a slight shift to positive correlations. The mean correlation coefficient is 0.04. We have verified that the distribution does not depend on year and is the same for the quiet/active Sun. Figure 5 gives examples of flux measurements at two frequencies with positive correlation. In the case of the quiet Sun, the flux varies little and the correlation is low. In the case of a noise storm, despite the difference between emission intensities, the flux behavior at different frequencies is the same and $R=0.97$. We have found that except for two days with particularly intense noise storms (one of them is the storm in Figure 5) the diurnal correlation does not depend on the mean daily flux. Analysis of individual days with high anticorrelation has shown that in Learmonth and IISR data there may be a diurnal variation introducing an error in measurements. To address this potential problem, we have carried out an autocorrelation analysis.

5. AUTOCORRELATION ANALYSIS OF DIURNAL FLUX VARIATIONS

Ideally, no diurnal variation and correlation are expected between solar flux measurements made on neighboring days. We have calculated the Pearson correlation between measurement series of each pair of consecutive observation days (autocorrelation with a one-day delay). Figure 6 on the left shows histograms of the correlation for the 161 and 245 MHz fluxes. Distribution shapes for different frequencies differ significantly, but a shift to positive correlations is observed in both cases ($R_{\text{mean}}=0.27$ for 161 MHz, $R_{\text{mean}}=0.44$ for 245 MHz). As examples of a high correlation $R>0.8$, comparisons between series of flux measurements on neighboring days at the corresponding frequency are shown on the right. In both cases, there is an obvious iterative diurnal variation in the data. Based on the shape of the correlation distribution and the method of measuring the flux with IISR, we can conclude that in part of the 161 MHz data series there is a diurnal variation associated with the error of determining the directional pattern. For the 245 MHz flux we assume that the shape of the correlation distribution consists of two modes: a mode near zero for measurements that do not correlate from day to day, and a mode with high correlation near $p=1$ for days with a significant diurnal variation. This assumption is confirmed by visual analysis of different Learmonth measurement series: most data with high autocorrelation has a pronounced diurnal variation (see Figure 6, the row for 245 MHz).

Figure 7 shows an autocorrelation value averaged over months and years. Monthly variations are insignificant and close to the general mean value for the corre-

sponding frequencies. Annual variations are more interesting. For the 161 MHz flux, the highest mean correlation occurred in 2015 (only for 14 days of observation); and the lowest, in 2017, yet the correlation changes little with time. The mean correlation for Learmonth data is high in 2006–2010 ($R_{\text{mean}}\approx 0.5$), decreases to $R_{\text{mean}}=0.15$ in 2011, and then increases to the maximum value $R_{\text{mean}}\approx 0.7$ in 2021 and 2022.

Simple threshold filtering of IISR and Learmonth data with high autocorrelation $R>0.8$ allowed us to increase the correlation coefficient of mean daily fluxes, presented in Section 3, by ~ 0.05 . Nevertheless, ratios between the correlation coefficients for different combinations of frequencies (see correlation matrices in Figure 3) changed little.

6. DISCUSSION

New additional methods for correcting the IISR directional pattern have expanded the number of available measurements of the 161 MHz solar flux as compared to previous works [Setov et al., 2020]. Despite their being sparse with large gaps, the IISR data provides information about a rarely studied part of the solar emission spectrum. However, the autocorrelation analysis has shown the presence of an error due to the unexplained diurnal variation associated with the influence of the antenna pattern. Nonetheless, in previous studies the error was higher because the antenna pattern model was used which did not display significant frequency variations in the range of solar observation. In the future, we plan to reduce the measurement error by improving antenna models and the IISR directional pattern, as well as by increasing the number of measurements due to observations in subsequent years.

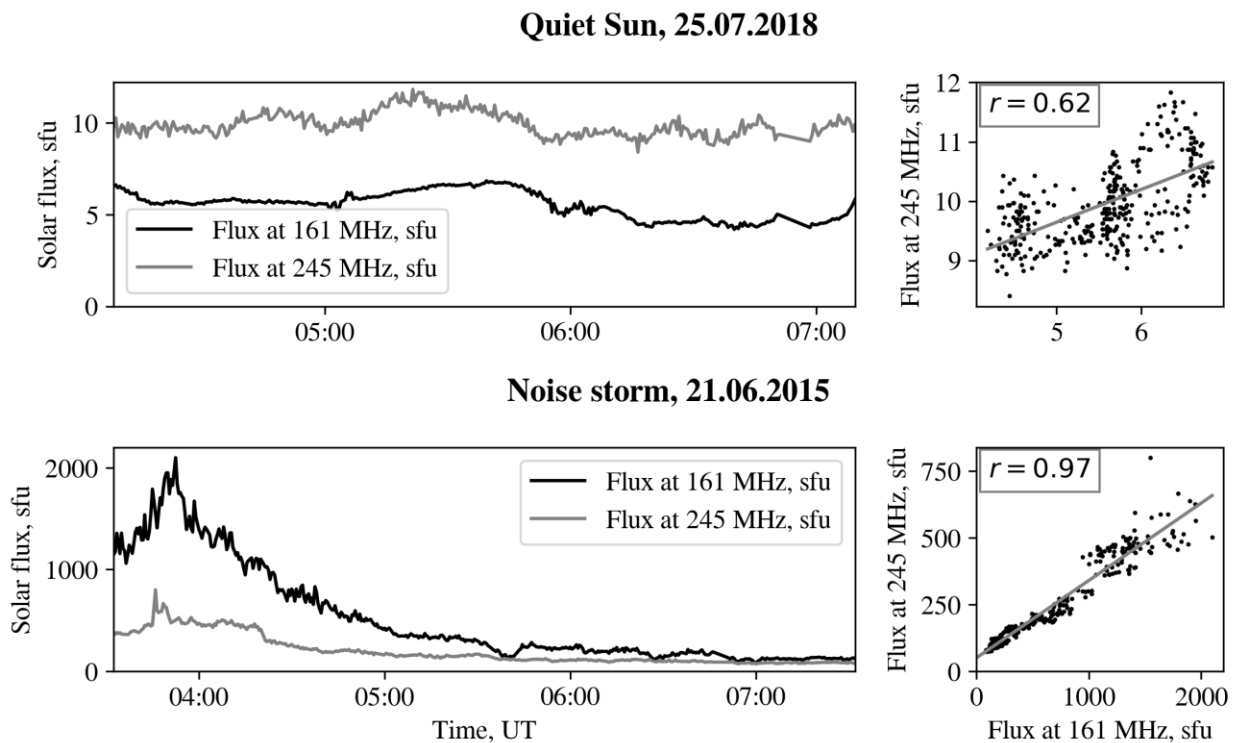


Figure 5. Comparison between variations in 161 and 245 MHz fluxes in the quiet Sun and during a noise storm

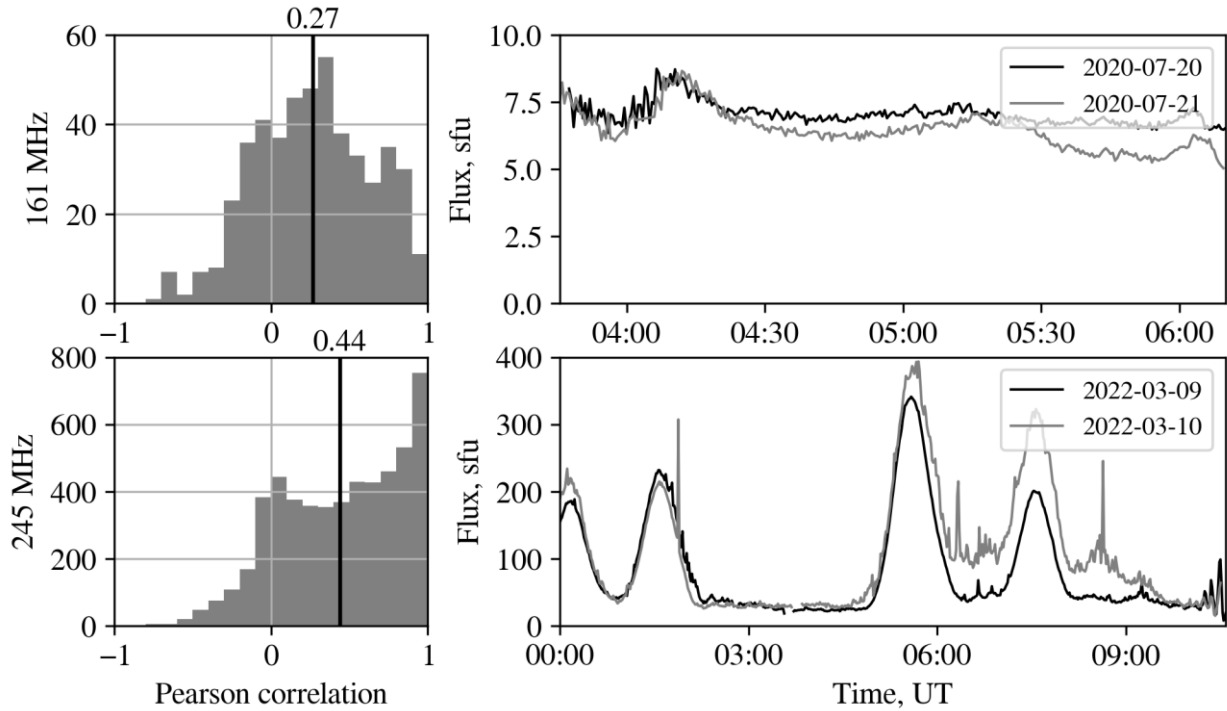


Figure 6. Autocorrelation distribution for neighboring days (left). The vertical line marks the mean value. Diurnal variations in fluxes of neighboring days with a high correlation coefficient (right). Top panels for 161 MHz, bottom panels for 245 MHz

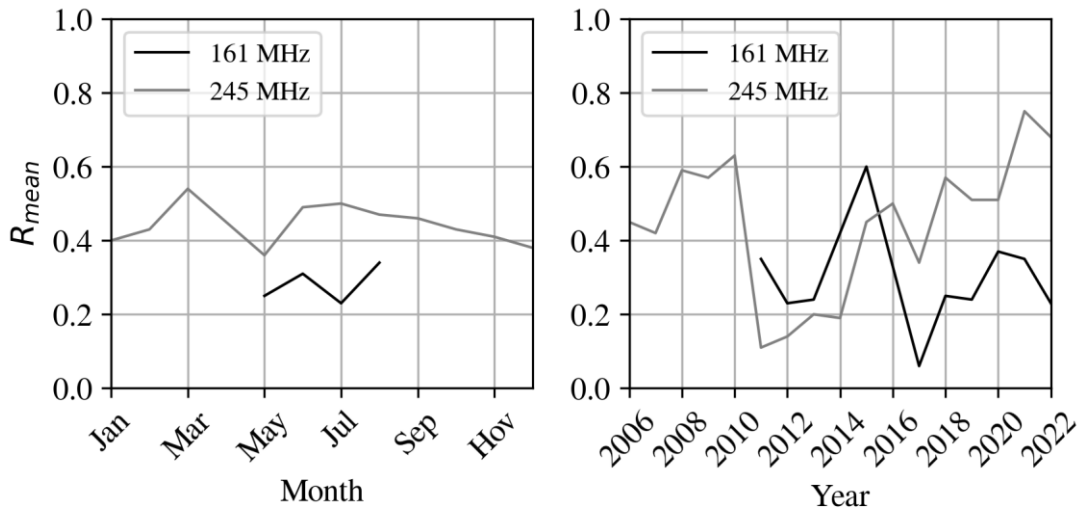


Figure 7. Daily flux correlation coefficient R averaged over months (left) and years (right) for neighboring days

The background solar flux at 161 and 245 MHz, detected by IISR and at Learmonth, takes values close to the model ones at solar minimum. This is primarily an indicator of the reliability of IISR and Learmonth data calibration. The mean annual flux follows changes in the sunspot number during a solar cycle. There is a positive, albeit low, correlation between the mean daily flux and $F10.7$ (varies from 0.26 to 0.79 depending on the method of calculating correlation). The Spearman correlation between the VHF flux and $F10.7$ is higher than the Pearson correlation, which suggests that the dependence is non-linear. Study of the correlation between different data percentiles has shown that a significant increase in the 161 and 245 MHz fluxes is not accompanied by significant changes in the $F10.7$ flux. On average, the correlation between 161 MHz and $F10.7$ is by ~ 0.08 higher than that between 245 MHz

and $F10.7$. Since there is no physical justification for this, we believe that this difference relates to the quality of measurements. The correlation with the sunspot number is lower than that with $F10.7$. This might be due to the fact that the sunspot number takes a constant zero value when the Sun is quiet, whereas $F10.7$ may vary.

Contrary to expectations, the correlation between 161 and 245 MHz is on average lower than that between 161 MHz and $F10.7$, as well as between 245 MHz and $F10.7$, despite the proximity of meter-wave frequencies. Some series of daily measurements during noise storms show a clear high correlation through which the Pearson correlation takes a maximum value $R=0.71$ when all available data is used. Yet, if we discard these rare storms, the correlation decreases to 0.4–0.6. Calibration of the IISR and Learmonth power is a linear transfor-

mation and hence it should not change the correlation coefficient. In the absence of any physical justification, we attribute this discrepancy to measurement errors. Note that the Learmonth data also showed a relatively low correlation coefficient (0.6–0.8) with data from other RSTN stations [Giersch, Kennewell, 2022].

The distribution of the correlation between diurnal variations in the 161 and 245 MHz fluxes is slightly shifted to positive direction. Some days feature a high correlation, especially during long radio storms, but most data series are not correlated. Autocorrelation analysis has revealed that there is a diurnal variation in the data, which is part of the reason for the negative correlation of daily series. We believe that the diurnal variation in the IISR data appears due to errors in correcting the antenna pattern. For the Learmonth data, however, the nature of the diurnal variation is unclear. A large number of days, especially in recent years, seem to contain intense slow variations with the same everyday behavior. We have not found any mention of the diurnal variation in other papers that use Learmonth data. In a follow-up work with both IISR and Learmonth flux measurements, it is necessary to develop techniques that will show the presence or absence of the diurnal variation.

CONCLUSION

We have carried out a comparative correlation analysis of solar flux measurements made with IISR in radio astronomy mode at 161 MHz and at RSTN Learmonth Observatory at 245 MHz. The IISR data covers 2011–2022 and, due to the correction of the antenna pattern, includes at least 56 observation days every year from 2017 to 2022 with a duration from 1 hr. Absolute measurements of the total flux in VHF complement the spectral measurements made with numerous but low-sensitive spectropolarimeters. In this paper, we have examined flux variations during a solar cycle and separately estimated the distribution of the quiet-Sun background flux. The quiet-Sun fluxes at 161 and 245 MHz have been demonstrated to agree with model calculations. The analysis has shown a correlation between the VHF flux and the $F_{10.7}$ index, but the correlation between 161 and 245 MHz was lower than that with $F_{10.7}$. Possible reasons are the error in estimating the correlation due to the difference between Learmonth and IISR data sets, as well as the presence of a diurnal variation in part of Learmonth data.

We have found a correlation between diurnal variations in fluxes for neighboring days. The presence of the correlation is interpreted as a result of measurement error. For IISR, this error may be due to an error in estimating the radar directional pattern. In follow-up works, we plan to develop a method for correcting the diurnal variation and reducing the error, as well as to analyze noise storms at 161 MHz with high time resolution.

The work was financially supported by the Russian Science Foundation (Grant No. 22-17-00146) [<https://rscf.ru/project/22-17-00146/>] in terms of developing the data processing method and analyzing the results. The work was financially supported by the Ministry of Science

and Higher Education of the Russian Federation in terms of observations. We have used measurement data from the Unique Research Facility "Irkutsk Incoherent Scatter Radar" [<http://ckp-rf.ru/usu/77733/>]. Data on the solar flux measured at Learmonth Observatory is available on the FTP server of the Bureau of Meteorology of the Australian Government [<ftp://ftp-o.ut.sws.bom.gov.au>].

REFERENCES

- Benz A.O. Radio emission of the quiet Sun. *Landolt Börnstein*. 2009, vol. VI/4B, pp. 1–13. DOI: [10.1007/978-3-540-88055-4_5](https://doi.org/10.1007/978-3-540-88055-4_5).
- Borkowski K.M. The quiet Sun brightness temperature at 127 MHz. *Solar Phys.* 1982, vol. 81, pp. 207–215. DOI: [10.1007/BF00151297](https://doi.org/10.1007/BF00151297).
- Giersch O., Kennewell J. Analysis of the radio solar telescope network's noon flux observations over three solar cycles (1988–2020). *Radio Sci.* 2022, vol. 57, e2022RS007456. DOI: [10.1029/2022RS007456](https://doi.org/10.1029/2022RS007456).
- Hamini A., Auxepales G., Birée L., Kenfack G., Kerdraon A., Klein K.-L., et al. ORFEES — a radio spectrograph for the study of solar radio bursts and space weather applications. *J. Space Weather Space Clim.* 2021, vol. 11, no. 57. DOI: [10.1051/swsc/2021039](https://doi.org/10.1051/swsc/2021039).
- Iwai K., Tsuchiya F., Morioka A., Misawa H. IPRT/AMATERAS: A New Metric Spectrum Observation System for Solar Radio Bursts. *Solar Phys.* 2012, vol. 277, pp. 447–457. DOI: [10.1007/s11207-011-9919-y](https://doi.org/10.1007/s11207-011-9919-y).
- Kashapova L.K., Kolotkov D.Y., Kupriyanova E.G., Kudriavtseva A., Chengming Tan, Reid H. Common origin of quasi-periodic pulsations in microwave and decimetric solar radio bursts. *Solar Phys.* 2021, vol. 296, no. 185, pp. 1–16. DOI: [10.1007/s11207-021-01934-x](https://doi.org/10.1007/s11207-021-01934-x).
- Lantos P. Low frequency observations of the quiet Sun: a review. *Proc. Nobeyama Symposium "Solar Physics with Radio Observations"*. 1998, pp. 11–24.
- Lu L., Liu, S., Song Q., Ning Z. Calibration of Solar Radio Spectrometer of the Purple Mountain Observatory. *Chinese Astron. Astrophys.* 2015, vol. 39, pp. 497–511. DOI: [10.1016/j.chinastron.2015.10.007](https://doi.org/10.1016/j.chinastron.2015.10.007).
- Medvedev A.V., Potekhin A.P. Irkutsk Incoherent Scatter Radar: history, present and future. *History of Geo- and Space Sciences*. 2019, vol. 10, pp. 215–224. DOI: [10.5194/hgss-10-215-2019](https://doi.org/10.5194/hgss-10-215-2019).
- Oberoi D., Sharma R., Rogers A.E.E. Estimating solar flux density at low radio frequencies using a sky brightness model. *Solar Phys.* 2017, vol. 292, 75, pp. 1–16. DOI: [10.1007/s11207-017-1096-1](https://doi.org/10.1007/s11207-017-1096-1).
- Potekhin A.P., Medvedev A.V., Zavorin A.V., Kushnarev D.S., Lebedev V.P., Lepetaev V.V., Shpynev B.G. Recording and control digital systems of the Irkutsk Incoherent Scatter Radar. *Geomagnetism and Aeronomy*. 2009, vol. 49, no. 7, pp. 1011–1021. DOI: [10.1134/S0016793209070299](https://doi.org/10.1134/S0016793209070299).
- Setov A.G., Globa M.V., Medvedev A.V., Vasilyev R.V., Kushnarev D.S. First results of absolute measurements of solar flux at the Irkutsk Incoherent Scatter Radar (IISR). *Solar-Terr. Phys.* 2018, vol. 4, Iss. 3, pp.24–27. DOI: [10.12737/stp-43201804](https://doi.org/10.12737/stp-43201804).
- Setov A.G., Kushnarev D.S., Vasilyev R.V., Medvedev A.V. Long-term solar flux observations with Irkutsk Incoherent Scatter Radar (IISR) in 2011–2019. *Solar-Terr. Phys.* 2020, vol. 6, Iss. 3, pp. 29–33. DOI: [10.12737/stp-63202004](https://doi.org/10.12737/stp-63202004).
- Spearman C. The Proof and Measurement of Association between Two Things. *The American J. Psychology*. 1904, vol. 15, no. 1, pp. 72–101. DOI: [10.2307/1412159](https://doi.org/10.2307/1412159).

Tan C., Yan Y., Tan B., Fu Q., Liu Y., Xu G. Study of calibration of solar radio spectrometers and the quiet-Sun radio emission. *Astrophys. J.* 2015, vol. 808, 61. DOI: [10.1088/0004-637X/808/1/61](https://doi.org/10.1088/0004-637X/808/1/61).

Tapping K.F. The 10.7 cm solar radio flux ($F_{10.7}$). *Space Weather*. 2013, vol. 11, pp. 394–406. DOI: [10.1002/swe.20064](https://doi.org/10.1002/swe.20064).

Vocks C., Mann G., Breitling F., Bisi M., Dąbrowski B., Fallows R., et al. LOFAR observations of the quiet solar corona. *Astron. Astrophys.* 2018, vol. 614, no. A54, pp. 1–9. DOI: [10.1051/0004-6361/201630067](https://doi.org/10.1051/0004-6361/201630067).

Zheng H., Tegmark M., Dillon J.S., Kim D.A., Liu A., Neben A., et al. An improved model of diffuse galactic radio emission from 10 MHz to 5 THz. *Monthly Notices Royal Astron. Soc.* 2016, vol. 464, no. 3, pp. 3486–3497. DOI: [10.1093/mnras/stw2525](https://doi.org/10.1093/mnras/stw2525).

URL: <https://www.sws.bom.gov.au/Solar/3/4> (accessed June 2, 2023).

URL: <https://rscf.ru/project/22-17-00146/> (accessed September 29, 2023).

URL: <http://ckp-rf.ru/usu/77733/> (accessed September 29, 2023).

URL: <ftp://ftp-out.sws.bom.gov.au> (accessed June 2, 2023).

Original Russian version: Setov A.G., Kushnarev D.S., published in *Solnechno-zemnaya fizika*. 2023. Vol. 9. Iss. 4. P. 54–62. DOI: [10.12737/szf-94202306](https://doi.org/10.12737/szf-94202306). © 2023 INFRA-M Academic Publishing House (Nauchno-Izdatelskii Tsentr INFRA-M)

How to cite this article

Setov A.G., Kushnarev D.S. Correlation analysis of solar flux absolute measurements at 161 and 245 MHz. *Solar-Terrestrial Physics*. 2023. Vol. 9. Iss. 4. P. 46–54. DOI: [10.12737/stp-94202306](https://doi.org/10.12737/stp-94202306).